From Bright Windows to Dark Spots: The Evolution of Melt Pond Optical Properties during Refreezing

Philipp Anhaus[1,1], Christian Katlein[1,1], Marcel Nicolaus[2,2], Mario Hoppmann[3,3], and Christian Haas[4,4]

[1]Alfred-Wegener-Institut Helmholtz-Zentrum für Polar- und Meeresforschung
[2]Alfred Wegener Institute
[3]AWI, Germany
[4]AWI

November 30, 2022

Abstract

Melt ponds have a strong impact on the Arctic surface energy balance and the ice-associated ecosystem because they transmit more solar radiation compared to bare ice. In the existing literature, melt ponds are considered as bright windows to the ocean, even during freeze-up in autumn. In the central Arctic during the summer-autumn transition in 2018, we encountered a situation where more snow accumulated on refrozen melt ponds compared to the adjacent bare ice, leading to a reduction in light transmittance of the ponds even below that of bare ice. Supporting results from a radiative transfer model suggest that melt ponds with a snow cover >0.04 m lead to lower light transmittance than adjacent bare ice. This scenario has not been described in the literature before, but has potentially strong implications for example on autumn ecosystem activity, oceanic heat budget and thermodynamic ice growth.

From Bright Windows to Dark Spots: Snow Cover Controls Melt Pond Optical Properties during Refreezing

P. Anhaus[1*], C. Katlein[1], M. Nicolaus[1], M. Hoppmann[1], C. Haas[1,2]

[1]Alfred-Wegener-Institut Helmholtz-Zentrum für Polar- und Meeresforschung, Bremerhaven, Germany

[2]Department of Environmental Physics, University of Bremen, Bremen, Germany

*Corresponding author: Philipp Anhaus (philipp.anhaus@awi.de)

Key Points:

- Refrozen melt ponds may collect a thicker snow cover compared to bare sea ice due to their recessed topography
- Such snow-covered melt ponds transmit less light compared to bare ice of similar type
- This scenario has not been documented before and should be accounted for in studies involving light in a refreezing Arctic Ocean

Word count = 4232

Abstract

Melt ponds have a strong impact on the Arctic surface energy balance and the ice-associated ecosystem because they transmit more solar radiation compared to bare ice. In the existing literature, melt ponds are considered as bright windows to the ocean, even during freeze-up in autumn. In the central Arctic during the summer-autumn transition in 2018, we encountered a situation where more snow accumulated on refrozen melt ponds compared to the adjacent bare ice, leading to a reduction in light transmittance of the ponds even below that of bare ice. Supporting results from a radiative transfer model suggest that melt ponds with a snow cover >0.04 m lead to lower light transmittance than adjacent bare ice. This scenario has not been described in the literature before, but has potentially strong implications for example on autumn ecosystem activity, oceanic heat budget and thermodynamic ice growth.

Plain Language Summary

Arctic sea ice is covered with snow during autumn, winter and spring. During summer, melt ponds evolve in response to surface melting. After snow fall starts again in autumn, these ponds can be filled with a lot of snow compared to bare ice because of their recessed surface. Indeed, during an expedition close to the North Pole in summer and autumn 2018, we measured a thick snow cover on ponds. This thick snow cover reduced the light availability underneath the ponds to levels below that underneath adjacent bare ice. This is a surprising finding, because it is different from the established theory of high light availability underneath melt ponds during both summer and autumn and how this is described in most computer models. It has consequences for our

43 understanding of the ice-associated ecosystem (organisms that live in and under sea ice). It might
44 also impact the mass and energy balance of central Arctic sea ice during summer-autumn transition
45 when new sea ice starts forming.

46

47 **1 Introduction**

48 Snow controls the optical properties and, thus, regulates the energy as well as the mass balance of
49 sea ice because of its high reflectivity (Grenfell and Maykut, 1977) and insulation (e.g., Sturm et
50 al., 1997). The snow cover of Arctic sea ice is highly variable in time and space (Webster et al.,
51 2018). The rougher the sea ice topography the more snow accumulates (Sturm et al, 2002; Massom
52 et al., 1997), for example at the lee sides of pressure ridges (Webster et al., 2018), at windward
53 sides of snow dunes (Dadic et al., 2013) and within the depression of melt ponds (Perovich et al.,
54 2003). In turn, the distribution of snow, especially snow dunes, influence melt pond formation
55 (Petrich et al., 2012a; Polashenski et al., 2012). Melt ponds also play a key role for the surface
56 energy budget (Nicolaus et al., 2012) and the mass balance of sea ice (Flocco et al., 2015), as well
57 as for the ice- and ocean-associated ecosystem (Arrigo, 2014). In general, in August-September
58 the melt pond coverage peaks (Perovich et al., 2002) and open and mature ponds evolve towards
59 refrozen and snow-covered ponds (Perovich et al., 2009). The areal fraction of melt ponds on
60 Arctic first-year ice is up to 53% and 20-38% on multi-year ice (e.g., Webster et al., 2015; Nicolaus
61 et al., 2012; Perovich et al., 2003; Fetterer and Untersteiner, 1998). This fraction has been shown
62 to increase from 15% to 35% for multi-year ice based on observations (Perovich et al., 2009) and
63 from 11% to 34% for the entire Arctic based on model simulations (Schröder et al., 2014). The
64 amount of radiation that is reflected back to the atmosphere is significantly reduced for melt ponds
65 compared to bare ice (e.g., Nicolaus et al, 2012). Instead, a considerable amount of radiation is

absorbed by and transmitted through melt ponds (e.g., Katlein et al., 2015; Nicolaus et al., 2012; Ehn et al., 2011; Light et al., 2008; 2015). Consequently, the ice underlying the melt ponds warms and can thin faster than bare ice during snow-free summer (Flocco et al., 2015; Hanson, 1965; Untersteiner, 1961).

The translucent melt ponds are often considered as bright windows in Arctic sea ice, even during autumn when their surface refreezes. The formation and occurrence of under-ice phytoplankton blooms are highly dependent on snow and sea ice conditions and, thus, on the under-ice light field (Ardyna et al., 2020). An Arctic-wide increase in the occurrence of the blooms was partly explained by the increasing fraction of melt ponds (Horvat et al., 2017). Lee et al. (2015) showed that ice algal masses accumulate in and under refrozen and snow-free melt ponds that favor higher light availability. They argue that algal accumulations in autumn can provide an important food source for higher trophic animals before and during winter.

This study documents a situation where a thicker snow cover accumulates on melt ponds compared to bare ice after snow fall starts in autumn. The thicker snow cover reduces the light availability under melt ponds to levels lower than under adjacent bare ice. Using data collected in the central Arctic close to the geographic North Pole during the transition from summer to autumn in 2018, we investigate the effect of snow accumulated on the refrozen melt ponds on the under-ice light availability. We compare two datasets that represent the summer and autumn conditions, which mainly consist of snow depth and ice thickness measurements, along with aerial images and under-ice transmittance data from a remotely operated vehicle (ROV). We apply a radiative transfer model to calculate an estimate for the snow accumulation threshold necessary for the light level to be lower under melt ponds compared to bare ice.

2 Materials and Methods

2.1 Study Site

The data presented in this study were collected during the Arctic Ocean 2018 MOCCHA – ACAS – ICE campaign (short: AO18) onboard the Swedish icebreaker *Oden*. During this campaign, a temporary ice camp was set up on drifting, ponded multi-year ice close to the geographic North Pole between 14 August and 14 September 2018. Snow depth, total sea ice thickness (ice thickness plus snow depth) and transmitted irradiance were measured in an area of approximately 100 m x 100 m (Figure 1). Marker poles (M0 to M23) were deployed under the ice to facilitate ROV navigation and to obtain a better co-location of the data. The mean ice thickness of bare ice was 1.9 m and of the ice underlying the melt ponds 1.7 m (Table S2). Melt ponds were on average 0.3 m deep. Here we focus on two main datasets: measurements performed between 17 and 24 August represented summer conditions which were characterized by open or only slightly refrozen melt ponds and no snow cover, whereas measurements performed between 13 and 14 September represented autumn conditions which were characterized by refrozen and snow-covered melt ponds.

2.2 Snow Depth and Sea Ice Thickness

Snow depth point measurements with a horizontal spacing of 1 to 3 m and an accuracy of 0.01 m were obtained on the (pristine) study area using a Magna Probe (Snow-Hydro, Fairbanks, AK, USA, Sturm and Holmgren, 2018). On snow-covered bare ice the Magna Probe likely penetrates into the underlying surface scattering layer (SSL) leading to an overestimate in snow depth. The GPS position of each measurement was recorded by an integrated GPS with an accuracy of 2.5 m (Sturm and Holmgren, 2018).

Total (sea ice plus snow) thickness was determined using a ground-based electromagnetic induction sounding device (GEM-2, Geophex Ltd, Raleigh, NC, USA, Hunkeler et al., 2015) using the in-phase signal at a frequency of 18.33 kHz. The GEM-2 was placed on a sledge and dragged across the study area in a grid pattern at the very end of the campaign. The accuracy of the total thickness measurements is ± 0.1 m (Hunkeler et al., 2015). Finally, ice thickness was calculated from total thickness by subtracting the (interpolated) snow depths. GPS positions of snow depth and ice thickness measurements were subsequently corrected for ice drift using GPS recorders placed at the acoustic transponder locations to enable co-location with the transmittance measurements.

In addition, in situ snow depth, ice thickness, draft, freeboard, and melt pond depth were measured in drill holes at the marker locations using a tape measure on 17 August.

2.3 Under-Ice Transmittance

Horizontal transects of under-ice spectral irradiance were measured by a RAMSES-ACC hyper-spectral radiometer (TriOS GmbH, Rastede, Germany). The radiometer was mounted on a M500 ROV (Ocean Modules, Åtvidaberg, Sweden, Katlein et al., 2017). The ROV was lowered into the water through a 2 x 2 m hole in the ice covered by a tent next to the study area (Figure 1).

The light transmittance was calculated by wavelength-integrating the transmitted irradiance from 350 to 920 nm and normalizing by the incident downwelling planar irradiance recorded by an upward-looking reference sensor at the surface. The data were filtered for ROV pitch, roll and depth, and noise was filtered from the spectra. Using the photosynthetically active radiation (400 to 700 nm) did not lead to qualitatively different results and conclusions in this work, and is thus not further considered here.

For under-ice navigation, the ROV was equipped with an acoustic long baseline positioning system (Pinpoint 1500 Linkquest, San Diego, CA, USA). We manually post-processed the ROV position to remove distortions caused by calibration uncertainties.

2.4 Aerial Images

Oblique aerial images were obtained during a helicopter flight on 23 August (summer) and by a drone on 13 September (autumn). Those were used to retrieve the geographic coordinates of the melt ponds. The images were corrected for camera perspective and georeferenced using the marker locations measured by a terrestrial laser scanner (VZ-400i, RIEGL, Horn, Austria). Melt ponds in the image were detected using a simple threshold criterion. All pixels within the study area where $\text{mean}(R,G,B) < 70 + 0.5 \cdot B$ (Katlein et al., 2015) were classified as melt ponds, with R, G, B representing the integer values of the respective channels of the RGB color space (R=700 nm, G=525 nm, B=450 nm). We added a 2 m buffer by image dilation to account for horizontal light spreading (Ehn et al., 2011) and uncertainties of the ROV position.

2.5 Radiative Transfer Model

We modelled broadband reflection and under-ice transmittance using the radiative transfer model DORT2002 version 3.0 (Edström, 2005; Katlein et al., 2021). The model uses a discrete ordinate model geometry and is implemented in the MATLAB™ software. The ice geometry was approximated by three layers each for bare ice and melt ponds (Table S1): The bare ice consisted of the interior sea ice underlying a SSL with a freshly fallen snow layer of varying thickness on top. The melt ponds consisted of interior sea ice underlying the melt pond overlain by a snow layer of varying thickness. For simplicity, the situation without any snow will be referred to as “summer”

conditions whereas the snow covered scenario is referred to as “autumn” conditions. We used typical inherent optical properties for multi-year ice (Katlein et al., 2021; Perron et al., 2021).

3 Results and Discussion

3.1 Evolution of the Snow Cover in the Transition from Summer to Autumn

Figure 1 illustrates the distribution of melt ponds and bare ice and their surface properties during the transition from summer to autumn in the study area.

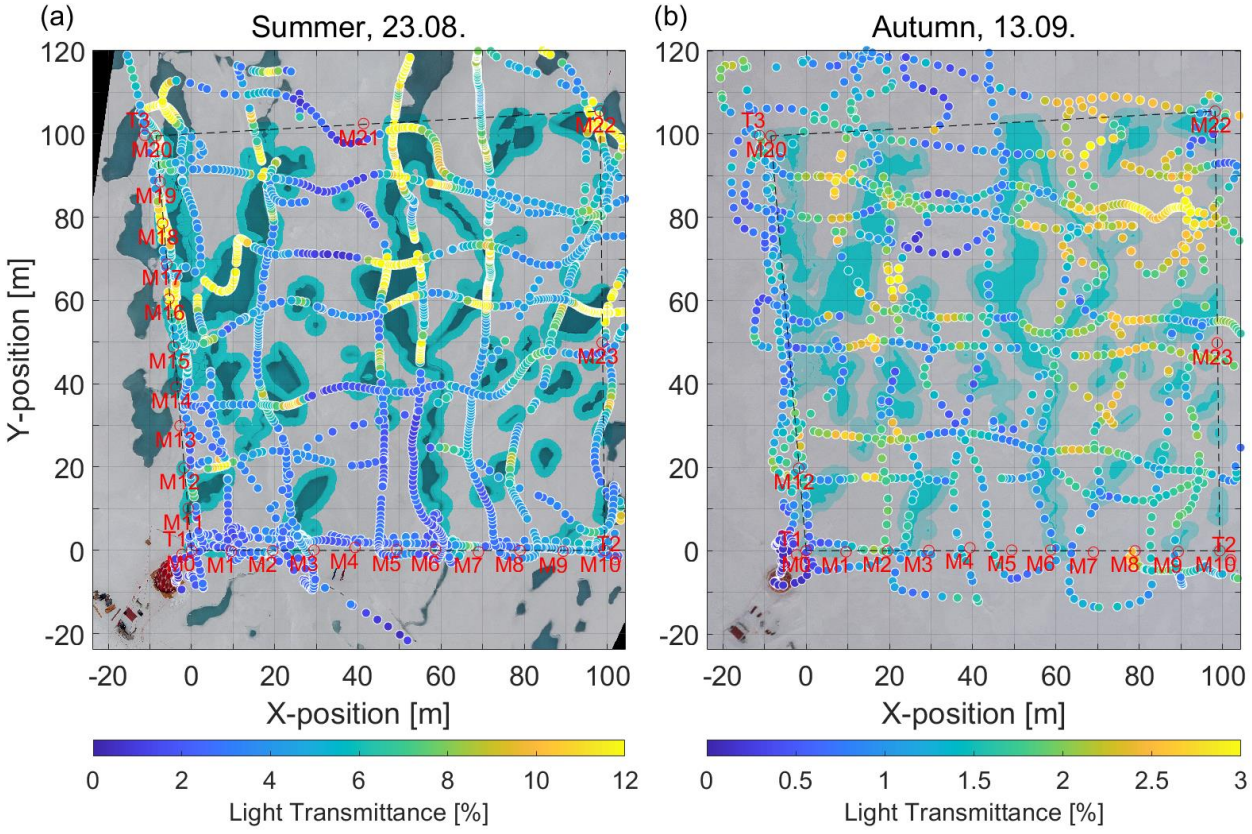

Figure 1: Light transmittance through ponded sea ice during the transition from (a) summer to (b) autumn. The data show ROV-based radiation measurements under (a) open melts ponds and (b) refrozen and snow-covered ponds. The background images are orthorectified aerial images acquired during (a) a low altitude helicopter flight and (b) a drone flight. Pixels within the study

171 area that were classified as melt pond and used for further analysis are colored in blue. The melt
172 ponds in (b) were refrozen and snow-covered but marked blue for illustration purposes. The edges
173 around the melt ponds in (a) and (b) were dilated by a buffer of about 2 m. This area is indicated
174 by a brighter blue. Red labels indicate the marker (M) and transponder locations (T). The ROV
175 tent and control hut are visible on the lower left corners of the images. Note the different range in
176 transmittance in (a) and (b).
177

178 On 23 August, the melt ponds were generally still open but in parts slightly refrozen at the surface
179 (Figures 1a and S1). No significant snow fall occurred prior to 29 August (Vüllers et al., 2019),
180 however a SSL of deteriorated ice with a mean thickness of 0.07 m was present. The passage of
181 low-pressure systems between 29 August and 15 September brought precipitation accompanied
182 by strong winds with speeds up to 13 ms^{-1} (Vüllers et al., 2019). This wind speed exceeded the
183 threshold of 8-10 ms^{-1} under which divergence of large amounts of drifting snow is favourable
184 (Van den Broeke and Bintanja, 1995). As a result, snow was deposited and re-distributed towards
185 and caught by the recessed and refrozen melt ponds and their edges (Figure S1, Fetterer &
186 Untersteiner, 1998; Perovich et al., 2003). This led to a higher mean snow accumulation on the
187 ponds (0.14 m) compared to on bare ice (0.11 m) as measured on 13 September (Figure 2a, Table
188 S2). On the melt ponds, higher snow depths were also much more frequently measured than on
189 bare ice (modes of 0.17 and 0.22 m, Figure 2a).

190 The snow mostly covered the visible surface signature of the ponds (Figure 1). However, the ponds
191 were still discernible because of their brighter appearance due to the higher snow depth compared
192 to the adjacent bare ice (Figure 1b).
193

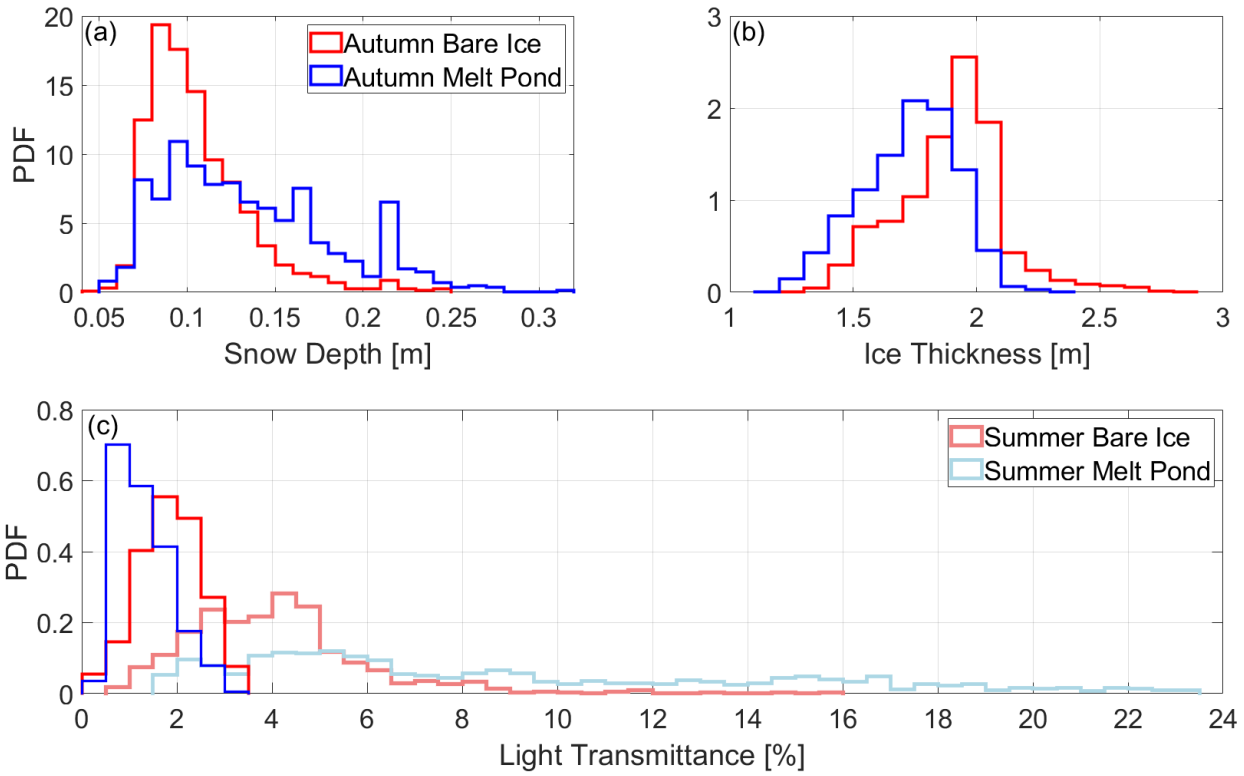

Figure 2: Histograms of measured (a) snow depth, (b) ice thickness, and (c) light transmittance of melt ponds and bare ice.

The higher snow depth on the melt ponds can have important implications on the sea ice mass balance related to the insulating effect of the snow cover (Sturm et al., 1997). Reduced heat loss (Maykut, 1978) and thermodynamic ice growth (Merkouriadi et al., 2017; Maykut, 1978) as well as delayed freeze-up of the liquid melt pond (Flocco et al., 2015) and induced bottom roughness are expected.

The refrozen surface of the melt ponds alone reduces the heat release from the ocean through the ice towards the atmosphere (Flocco et al., 2015). This hampers ice growth at both water-ice interfaces of the refreezing pond, as well as between the sea ice bottom and the ocean in the transition from autumn to winter. This can result in a delay of the complete freeze-up of the pond by up to 60 days (Flocco et al., 2015). A thinner ice cover is more vulnerable to dynamic and

warming events. The presence of a snow cover on top of the refrozen pond surface and the still liquid melt pond underneath are expected to amplify those effects (Perovich et al., 2003). As a result of the reduced thermodynamic growth of the sea ice underlying melt ponds compared to bare ice, a generally rougher bottom topography might result, affecting the mass, momentum, heat, and salt fluxes at the sea ice-ocean interface.

The exact evolution of the thicker snow cover on melt ponds during refreezing depends on the sequence of weather events. Whether or not more snow accumulates on the refrozen melt ponds than on adjacent bare ice is governed by the wind speed and snow drift regime during and after the snow fall, by the snow properties, and by the roughness of the refrozen surface. Falling and deposited snow needs to be re-distributed before it can accumulate on the topographically recessed and rougher pond surface. Wet and heavy snow is more resistant to erosion by wind than low-density dry snow (e.g., Colbeck, 1979; Massom et al., 1997). For instance, new snow deposited on blue ice either by drifting or precipitation can hardly settle on the smooth and warm-temperate surface (Bintanja, 1999; Van den Broeke and Bintanja, 1995). In case downwind slopes are smooth, any snow that can temporarily accumulate is prevented from actually attaching to the surface (Dadic et al., 2013; Bintanja, 1999). On such surfaces, drifting snow is also prevented from becoming attached causing the wind to be stronger over the glazed surface than over the snow (Ferzzotti et al., 2002a). Furthermore, less snow will accumulate on smooth nilas with a low surface roughness (e.g., Sturm et al., 2002; Massom et al., 1997) than on surfaces with a higher surface roughness (e.g., Bintanja, 1999, Frezzotti, 2002b).

3.2 Optical Properties

The surface topography of the ponded ice cover was key in modulating spatial variability in snow depth and hence light transmittance: The presence of open melt ponds in summer and the variability in snow depth driven by the refrozen melt ponds in autumn also led to spatial and temporal variability in the under-ice light field. On 24 August, ROV-based mean and maximum transmittances of ponds (8.9% and 23.2%, respectively) were significantly higher than those of bare ice (4.1% and 15.5%, see also Figures 1a and 2c and Table S2). Histograms showed a bi-modal transmittance distribution of ponds and bare ice combined (Figure S2). The distribution also showed a characteristic long tail for ponds, indicating high spatial variability and different properties of the ponds. This distribution is typical for Arctic summer sea ice and results from the formation and development of the melt ponds (Katlein et al., 2015; 2019; Nicolaus et al., 2012; Schanke et al., 2021). The magnitudes of transmittance are similar to observations from Nicolaus et al. (2012) in the same region in August 2011. The maximum transmittance of the melt ponds also agrees to values found by Katlein et al. (2019).

Due to the new snow cover on top of both the refrozen melt ponds and the bare ice (Figure 1b), the transmittance of both melt ponds and bare ice decreased (Figures 1 and S2, Table S2). The spatial variability in the transmittance of both melt ponds and bare ice was significantly reduced in autumn while the long tail of the high transmittances diminished, with very few observations higher than 3% (Figures 2c and S2, Table S2). In summer, approximately 80% (25%) of the transmittance measurements were higher than 3% (9%). Due to stronger and more frequent snow fall events that started to occur from 28 August (Vüllers et al., 2021), only 1% (0%) of the transmittances measurements in autumn were higher than 3% (9%).

Lee et al. (2011) describe observations indicating that melt ponds remain bright windows even in autumn after refreezing, although they did not consider a snow cover. This implies that the transmittance of melt ponds remains higher than that of bare ice. Katlein et al. (2019) showed that the bi-modal structure of transmittance during summer is conserved even during the first weeks of freeze-up in mid of September. They further suggest that the transmittances of both melt ponds and bare ice decrease gradually and equally in the transition from summer to autumn. Snow and particular re-distribution were present during their transmittance measurements, however those were not adequately considered.

We observed a different scenario than Lee et al. (2011) and Katlein et al. (2019). A thicker snow cover accumulated on melt ponds compared to adjacent bare ice because of the pond's recessed topography. This led to a lower mean transmittance of melt ponds (1.3%) than of bare ice (1.8%) in autumn (Figures 1 and 2c, Table S2). The transmittance distribution showed two distinct modes of 1.0% and 2.0% associated with melt ponds and bare ice, respectively (Figure 2c, Table S2). Despite the reversal of the magnitude in the transmittance of melt ponds and bare ice, the spatial variability remained during autumn (Figure 1). This suggests that the spatial variability was still coupled to the ponds after snow accumulation and re-distribution and most likely also persisted into winter.

The transmittance of ridged ice with thicknesses up to 2.8 m was naturally still lower than that of the melt ponds (Figures S3b and 1b). Those measurements are included in the bare ice data and are represented in the tail of larger ice thicknesses in the histogram (Figure 2b).

This study provides first quantitative observations of lower light transmittance of melt ponds than of bare ice in autumn due to higher snow depths on the ponds. Major implications on the ice-

associated ecosystem and the energy balance of the sea ice might arise from those observations in case such a situation is viable for the entire Arctic which is very likely:

Lee et al. (2011) proposed that the soft refrozen surface of open melt ponds that are in connection with the ocean provides a fertile habitat for biomass in autumn. They pointed out that the biomass accumulated under the refrozen melt ponds serves as an important food source for higher trophic animals during the transition from autumn to winter and further into winter. However, as presented here, a snow cover significantly reduces the light availability in and under melt ponds in autumn, suggesting a limited suitability as habitat in terms of available light. Those observations lend support to a study by Lange et al. (2017), who found higher biomass values underneath hummocks on multi-year ice compared to adjacent level ice. Lange et al. (2017) attributed the differences in biomass accumulation to increased light availability under the hummocks resulting from a very thin or absent snow cover (Perovich et al., 2003). Our results and those of Lange et al. (2017) suggest that light conditions under sea ice in spring can already be initialized by melt pond coverage and snow distribution during autumn and may persist throughout winter.
Further, due to the common assumption that there is more light available under melt ponds than under bare ice also during autumn, processes and magnitudes of carbon uptake and biomass accumulation in models, might need to be adjusted with respect to our new observations.

Arndt and Nicolaus (2014) developed a parameterization to quantify the annual solar heat input through Arctic sea ice. For their calculations in autumn, they use for transmittances of melt ponds the fivefold (500%) of that of bare ice. However, our results showed that the modal transmittance of melt ponds is only half (50%) of that of bare ice once covered by the first snow (Table S2). Arndt and Nicolaus (2014) applied a constant summer mean melt pond fraction for multi-year ice of 29% (Rösel et al., 2012) and a transmittance of melt ponds for multi-year ice of 0.4%. They

297 estimated the solar heat input into the ocean in September to 0.69×10^{19} J. We adopted their
298 parameters but used the ratio of transmittances between melt ponds and bare ice as presented in
299 the present study. As a result, the solar heat input into the ocean decreased by 61%. This shows,
300 that despite the generally low solar energy fluxes in autumn compared to in summer (e.g., Perovich
301 et al., 2011; Arndt and Nicolaus, 2014), our described effect could have an important impact on
302 the energy budget if valid in the entire Arctic. In this regard, our results might also impact the
303 heat stored in the upper ocean, the interior sea ice structure, as well as internal and basal melting.

304

305 **3.3 Radiative Transfer Model**

306 For the effect described above, it is of interest to quantify the threshold snow depth that is necessary
307 to decrease the transmittance of melt ponds below that of bare ice. In order to determine this
308 threshold depth, we used the radiative transfer model DORT2002. Figure 3 summaries the
309 observations of this study in a schematic which are supported by simulated albedo and
310 transmittance. For the situation without snow (summer), both the simulated transmittances of melt
311 ponds and bare ice (9% and 4%, respectively) were very similar to our observations (8.9% and
312 4.1%, respectively, Figures 3 and S4, Table S2).

313

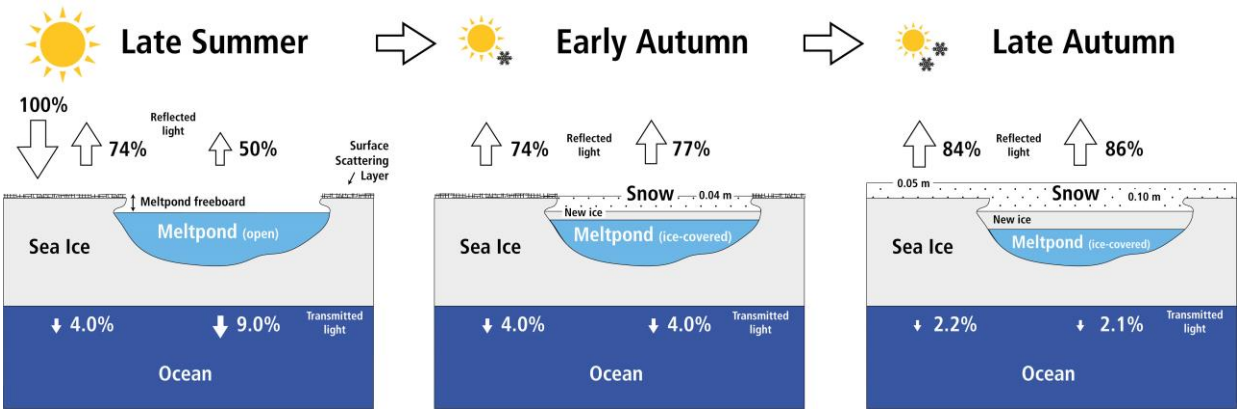

314

315 **Figure 3**: Simulated reflected light (albedo) and transmitted light (transmittance) as a function of
316 snow depth as modelled by DORT2002 for (left) snow-free melt ponds and bare ice, (middle)
317 snow-covered melt ponds and snow-free bare ice, and (right) snow-covered melt ponds and bare
318 ice. Properties used in the model are display in Table S1.
319
320 Incorporating an increasing snow cover from 0 to 0.20 m (autumn), our results yielded an
321 exponential decrease in the transmittances of both melt ponds and bare ice (Figure S4). For a snow
322 depth of approximately 0.04 m the transmittance of the melt ponds becomes equal to that of snow-
323 free bare ice (Figures 3 and S4). This is in agreement with the observations presented earlier which
324 showed that the transmittance of melt ponds was lower than that of bare ice for a 0.03 m higher
325 mean snow depth on the ponds (Table S2). Figure 3c illustrates that the transmittance of melt ponds
326 with a 0.10 m thick snow cover becomes lower than that of bare ice with a 0.05 m thick snow
327 cover.
328 In our simulations, the influence of the thin ice lid on the melt ponds on the transmittance was
329 neglected, as they were only partially existing, as for typical Arctic summer sea ice these are very
330 translucent and scattering is small (Lu et al., 2018), indicated by their blue-green color (Figure 1a).
331

332 **5 Summary**

333 Snow depth measurements on a ponded sea ice floe in the transition from summer to autumn reveal
334 that snow accumulation was on average 0.03 m higher on refrozen melt ponds than on adjacent
335 bare ice favored by the ponds recessed surface. Using under-ice radiation measurements from a
336 ROV we show that due to the thicker snow cover on the melt ponds the transmittance of the melt
337 ponds can become lower than that of bare ice. Those results imply that melt ponds cannot be

universally considered as bright windows of Arctic autumn sea ice. Computations from a radiative transfer model indicate that a snow cover with a depth >0.04 m accumulated on melt ponds result in transmittances of melt ponds becoming lower than that of snow-free bare ice. Our findings can have consequences for the autumn ecosystem activity, oceanic heat budget and thermodynamic ice growth if they can be observed in the entire Arctic.

Acknowledgments

This work was financed through the research programs PACES II and POF4 of the Alfred-Wegener-Institut Helmholtz-Zentrum für Polar- und Meeresforschung (AWI) and the Swedish Polar Research Secretariat (SPRS, grant no. AO18). Additional funding was received through the Diatom-ARCTIC project (NE/R012849/1; 03F0810A) as part of the Changing Arctic Ocean program (CAO), jointly funded by the UKRI Natural Environment Research Council (NERC) and the German Federal Ministry of Education and Research(BMBF). The ROV work was supported by the Helmholtz Infrastructure Initiative “Frontiers in Arctic marine Monitoring” (FRAM). We are thankful to the captain, crew and scientists onboard the *IB Oden*, as well as to the SPRS and AWI logistics for facilitating our participation in the AO18 expedition. Our special thanks go to Matthieu Labaste, Helen Czerski and Lars Lehnert for their field support, Ruzica Dadic for her advice on snow, and the polar bear guarding crew for keeping us safe.

Data availability

All data presented in this study are publicly available under the following DOIs:

ROV: https://doi.org/10.1594/PANGAEA.925698

Magna Probe and GEM2: https://doi.pangaea.de/10.1594/PANGAEA.934431

Aerial images: https://doi.org/10.5281/zenodo.5119094

Competing interest

The authors declare that they have no conflict of interest.

References

Ardyna, M., Mundy, C. J., Mills, M. M., Oziel, L., Grondin, L. L., Verin, G., et al. (2020). Environmental drivers of under-ice phytoplankton bloom dynamics in the Arctic Ocean. *Elementa: Science of the Anthropocene, 8*(30). doi:10.1525/elementa.430

Arndt, S., & Nicolaus, M. (2014). Seasonal cycle and long-term trend of solar energy fluxes through Arctic sea ice. *The Cryosphere, 8*(6). doi:10.5194/tc-8-2219-2014

Arrigo, K. R. (2014). Sea ice ecosystems. *Annual Review of Marine Science, 6*(1). doi:10.1146/annurev-marine-010213-135103

Bintanja, R. (1999). On the glaciological, meteorological, and climatological significance of Antarctic blue ice areas. *Reviews of Geophysics, 37*(3). doi:10.1029/1999rg900007

Colbeck, S. C. (1979). Sintering and compaction of snow containing liquid water. *Philosophical Magazine A, 39*(1). doi:10.1080/01418617908239272

Dadic, R., Mott, R., Horgan, H. J., & Lehning, M. (2013). Observations, theory, and modeling of the differential accumulation of Antarctic megadunes. *Journal of Geophysical Research: Earth Surface, 118*(4). doi:10.1002/2013jf002844

Edström, P. (2005). A Fast and Stable Solution Method for the Radiative Transfer Problem. *SIAM Rev., 47(3)*. doi:10.1137/s0036144503438718

Ehn, J. K., Papakyriakou, T. N., & Barber, D. G. (2008). Inference of optical properties from radiation profiles within melting landfast sea ice. *Journal of Geophysical Research, 113*(C09024). doi:10.1029/2007jc004656

Ehn, J. K., Mundy, C. J., Barber, D. G., Hop, H., Rossnagel, A., & Stewart, J. (2011). Impact of horizontal spreading on light propagation in melt pond covered seasonal sea ice in the Canadian Arctic. *Journal of Geophysical Research, 116*. doi:10.1029/2010jc006908

Fetterer, F., & Untersteiner, N. (1998). Observations of melt ponds on Arctic sea ice. *Journal of Geophysical Research: Oceans, 103*(C11). doi:10.1029/98jc02034

Frezzotti, M., Gandolfi, S., & Urbini, S. (2002a). Snow megadunes in Antarctica: Sedimentary structure and genesis. *Journal of Geophysical Research, 107*(D18). doi:10.1029/2001jd000673

Frezzotti, M., Gandolfi, S., La Marca, F., & Urbini, S. (2002b). Snow dunes and glazed surfaces in Antarctica: new field and remote-sensing data. *Annals of Glaciology, 34*. doi:10.3189/172756402781817851

Flocco, D., Feltham, D. L., Bailey, E., & Schroeder, D. (2015). The refreezing of melt ponds on Arctic sea ice. *Journal of Geophysical Research: Oceans, 120*(2). doi:10.1002/2014jc010140

Grenfell, T. C., & Maykut, G. A. (1977). The optical properties of ice and snow in the Arctic Basin. *Journal of Glaciology, 18*(80). doi:10.3189/S0022143000021122

Hanson, A. (1965). Studies of the Mass Budget of Arctic Pack-Ice Floes. *Journal of Glaciology, 5*(41). doi:10.3189/S0022143000018694

Hunkeler, P. A., Hoppmann, M., Hendricks, S., Kalscheuer, T., & Gerdes, R. (2016). A glimpse beneath Antarctic sea ice: Platelet layer volume from multifrequency electromagnetic induction sounding. *Geophysical Research Letters, 43*(1). doi:10.1002/2015gl065074

Katlein, C., Arndt, S., Nicolaus, M., Perovich, D. K., Jakuba, M. V., Suman, S., et al. (2015). Influence of ice thickness and surface properties on light transmission through Arctic sea ice. *Journal of Geophysical Research: Oceans, 120*(9). doi:10.1002/2015JC010914

Katlein, C., Schiller, M., Belter, H. J., Coppolaro, V., Wenslandt, D., & Nicolaus, M. (2017). A New Remotely Operated Sensor Platform for Interdisciplinary Observations under Sea Ice. *Frontiers in Marine Science, 4*. doi:10.3389/fmars.2017.00281

Katlein, C., Arndt, S., Belter, H. J., Castellani, G., & Nicolaus, M. (2019). Seasonal Evolution of Light Transmission Distributions Through Arctic Sea Ice. *Journal of Geophysical Research: Oceans, 124*(8). doi:10.1029/2018jc014833

Katlein, C., Valcic, L., Lambert-Girard, S., & Hoppmann, M. (2021). New insights into radiative transfer within sea ice derived from autonomous optical propagation measurements. *The Cryosphere, 15*(1). doi:10.5194/tc-15-183-2021

Lange, B. A., Flores, H., Michel, C., Beckers, J. F., Bublitz, A., Casey, J. A., et al. (2017). Pan-Arctic sea ice-algal chl a biomass and suitable habitat are largely underestimated for multiyear ice. *Global Change Biology, 23*(11). doi:10.1111/gcb.13742

Lee, S. H., McRoy, C. P., Joo, H. M., Gradinger, R., Cui, H., Yun, M. S., et al. (2011). Holes in Progressively Thinning Arctic Sea Ice Lead to New Ice Algae Habitat. *Oceanography, 24*(3). doi:10.5670/oceanog.2011.81

Light, B., Grenfell, T. C., & Perovich, D. K. (2008). Transmission and absorption of solar radiation by Arctic sea ice during the melt season. *Journal of Geophysical Research, 113*(C03023). doi:10.1029/2006jc003977

Light, B., Perovich, D. K., Webster, M. A., Polashenski, C., & Dadic, R. (2015). Optical properties of melting first-year Arctic sea ice. *Journal of Geophysical Research: Oceans, 120*(11). doi:10.1002/2015jc011163

Lu, P., Cao, X., Wang, Q., Leppäranta, M., Cheng, B., & Li, Z. (2018). Impact of a Surface Ice Lid on the Optical Properties of Melt Ponds. *Journal of Geophysical Research: Oceans, 123*(11). doi:10.1029/2018jc014161

Massom, R. A., Drinkwater, M. R., & Haas, C. (1997). Winter snow cover on sea ice in the Weddell Sea. *Journal of Geophysical Research: Oceans, 102*(C1). doi:10.1029/96jc02992

Maykut, G. A. (1978). Energy exchange over young sea ice in the central Arctic. *Journal of Geophysical Research, 83*(C7). doi:10.1029/JC083iC07p03646

Merkouriadi, I., Cheng, B., Graham, R. M., Rösel, A., & Granskog, M. A. (2017). Critical Role of Snow on Sea Ice Growth in the Atlantic Sector of the Arctic Ocean. *Geophysical Research Letters, 44*(20). doi:10.1002/2017gl075494

Nicolaus, M., Katlein, C., Maslanik, J., & Hendricks, S. (2012). Changes in Arctic sea ice result in increasing light transmittance and absorption. *Geophysical Research Letters, 39*(24). doi:10.1029/2012gl053738

Perovich, D. K. (1990). Theoretical estimates of light reflection and transmission by spatially complex and temporally varying sea ice covers. *Journal of Geophysical Research, 95*(C6). doi:10.1029/JC095iC06p09557

Perovich, D. K., Tucker III, W. B., & Ligett, K. A. (2002). Aerial observations of the evolution of ice surface conditions during summer. *Journal of Geophysical Research, 107*(C10). doi:10.1029/2000jc000449

Perovich, D. K., Grenfell, T. C., Richter-Menge, J. A., Light, B., Tucker III, W. B., & Eicken, H. (2003). Thin and thinner: Sea ice mass balance measurements during SHEBA. *Journal of Geophysical Research, 108*(C3). doi:10.1029/2001jc001079

Perovich, D. K., Grenfell, T. C., Light, B., Elder, B. C., Harbeck, J. P., Polashenski, C., et al. (2009). Transpolar observations of the morphological properties of Arctic sea ice. *Journal of Geophysical Research, 114*(C00A04). doi:10.1029/2008jc004892

Perovich, D. K., Richter-Menge, J. A., Jones, K. F., Light, B., Elder, B. C., Polashenski, C., et al. (2011). Arctic sea-ice melt in 2008 and the role of solar heating. *Annals of Glaciology, 52*(57). doi:10.3189/172756411795931714

Perron, C., Katlein, C., Lambert-Girard, S., Leymarie, E., Guinard, L.-P., Marquet, P., et al. (2021). Development of a Diffuse Reflectance Probe for In Situ Measurement of Inherent Optical Properties in Sea Ice, *The Cryosphere Discuss*., in review, doi:10.5194/tc-2021-104

Petrich, C., Eicken, H., Polashenski, C. M., Sturm, M., Harbeck, J. P., Perovich, D. K., et al. (2012a). Snow dunes: A controlling factor of melt pond distribution on Arctic sea ice. *Journal of Geophysical Research: Oceans, 117*(C09029). doi:10.1029/2012jc008192

Petrich, C., Nicolaus, M., & Gradinger, R. (2012b). Sensitivity of the light field under sea ice to spatially inhomogeneous optical properties and incident light assessed with three-dimensional Monte Carlo radiative transfer simulations. *Cold Regions Science and Technology, 73*. doi:10.1016/j.coldregions.2011.12.004

Polashenski, C., Perovich, D. K., & Courville, Z. (2012). The mechanisms of sea ice melt pond formation and evolution. *Journal of Geophysical Research: Oceans, 117*(C1). doi:10.1029/2011jc007231

Rösel, A., Kaleschke, L., & Birnbaum, G. (2012). Melt ponds on Arctic sea ice determined from MODIS satellite data using an artificial neural network. *The Cryosphere, 6*(2). doi:10.5194/tc-6-431-2012

Schröder, D., Feltham, D. L., Flocco, D., & Tsamados, M. (2014). September Arctic sea-ice minimum predicted by spring melt-pond fraction. *Nature Climate Change, 4*(5). doi:10.1038/nclimate2203

Sturm, M., Holmgren, J., König, M., & Morris, K. (1997). The thermal conductivity seasonal snow. *Journal of Glaciology, 43*(143). doi:10.3189/S0022143000002781

Sturm, M., Holmgren, J., & Perovich, D. K. (2002). Winter snow cover on the sea ice of the Arctic Ocean at the Surface Heat Budget of the Arctic Ocean (SHEBA): Temporal evolution and spatial variability. *Journal of Geophysical Research, 107*(C10). doi:10.1029/2000jc000400

Sturm, M., & Holmgren, J. (2018). An Automatic Snow Depth Probe for Field Validation Campaigns. *Water Resources Research, 54*(11). doi:10.1029/2018wr023559

Untersteiner, N. (1961). On the Mass and Heat Budget of Arctic Sea Ice. *Archiv für Meteorologie, Geophysik und Bioklimatologie, Serie A, 12*. doi:10.1007/BF02247491

Van den Broeke, M., & Bintanja, R. (1995). Summertime Atmospheric Circulation in the Vicinity of a Blue Ice Area in Queen Maud Land, Antarctica. *Boundary-Layer Meteorology, 72*(4). doi:10.1007/BF00709002

Vüllers, J., Achtert, P., Brooks, I. M., Tjernström, M., Prytherch, J., Burzik, A., et al. (2021). Meteorological and cloud conditions during the Arctic Ocean 2018 expedition. *Atmospheric Chemistry and Physics, 21*(1). doi:10.5194/acp-21-289-2021

Webster, M. A., Rigor, I. G., Nghiem, S. V., Kurtz, N. T., Farrell, S. L., Perovich, D. K., et al. (2014). Interdecadal changes in snow depth on Arctic sea ice. *Journal of Geophysical Research: Oceans, 119*(8). doi:10.1002/2014jc009985

Webster, M. A., Rigor, I. G., Perovich, D. K., Richter-Menge, J. A., Polashenski, C. M., & Light, B. (2015). Seasonal evolution of melt ponds on Arctic sea ice. *Journal of Geophysical Research: Oceans, 120*(9). doi:10.1002/2015jc011030

Webster, M. A., Gerland, S., Holland, M. M., Hunke, E., Kwok, R., Lecomte, O., et al. (2018). Snow in the changing sea-ice systems. *Nature Climate Change, 8*(11). doi:10.1038/s41558-018-0286-7

Geophysical Research Letters

Supporting Information for

From Bright Windows to Dark Spots: Snow Cover Controls Melt Pond Optical Properties During Refreezing

P. Anhaus[1*], C. Katlein[1], M. Nicolaus[1], M. Hoppmann[1], C. Haas[1,2]

[1]Alfred-Wegener-Institut Helmholtz-Zentrum für Polar- und Meeresforschung, Bremerhaven, Germany

[2]Department of Environmental Physics, University of Bremen, Bremen, Germany

*Corresponding author: Philipp Anhaus (philipp.anhaus@awi.de)

Contents of this file

Figure S1: Photograph as of 23 August illustrating that refrozen melt ponds have a recessed topographic position within the adjacent bare ice.

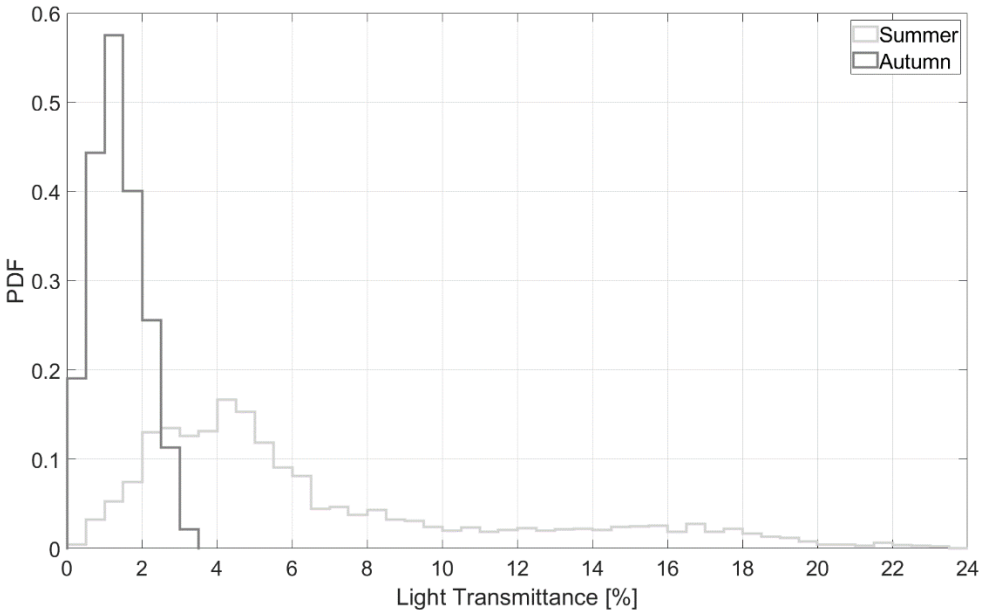

Figure S2: Histograms of light transmittance as measured on 24 August (summer) and 13 September (autumn) of melt ponds and bare ice combined.

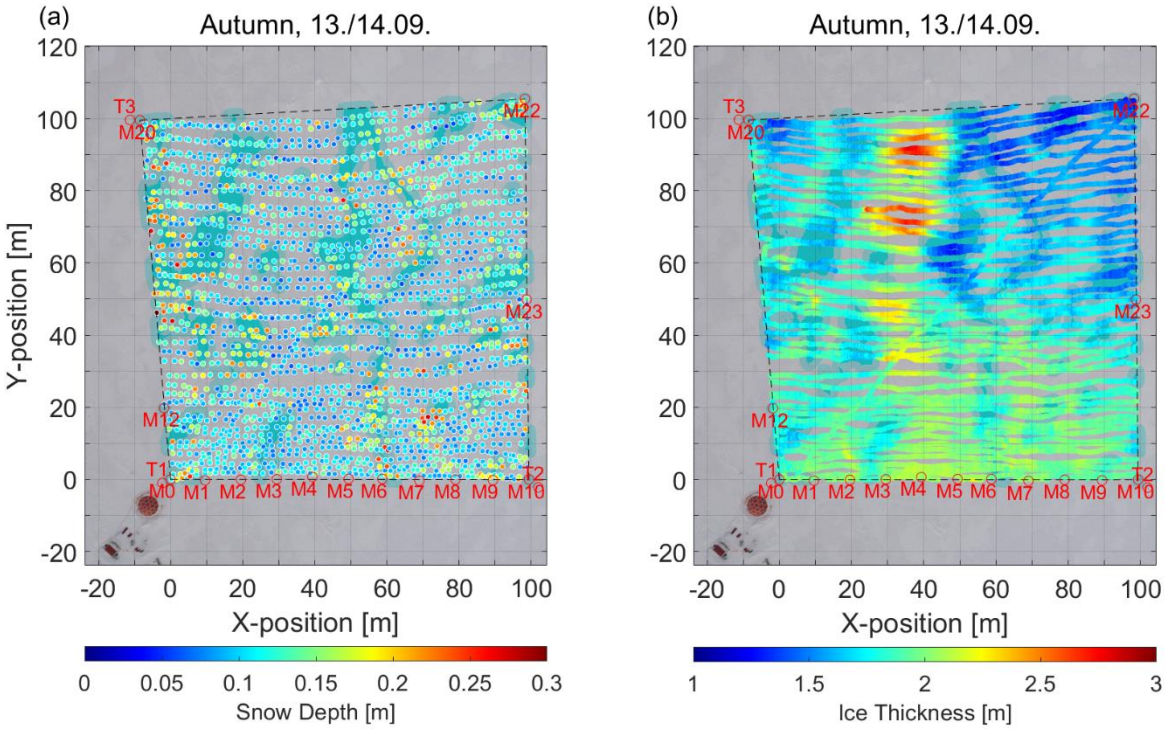

Figure S3: (a) Snow depth and (b) ice thickness on ponded sea ice as measured on 14 September (autumn). The background images are orthorectified aerial images acquired during a drone flight on 13 September. Pixels within the area of focus that were classified as melt pond during the summer are colored in light blue to illustrate the refrozen and snow-covered ponds during autumn. The edges around the melt ponds were dilated by a buffer of about 2 m. This area is indicated by a brighter blue. Red labels indicate the marker (M) and transponder locations (T). The ROV tent and control hut are visible on the lower left corners of the images.

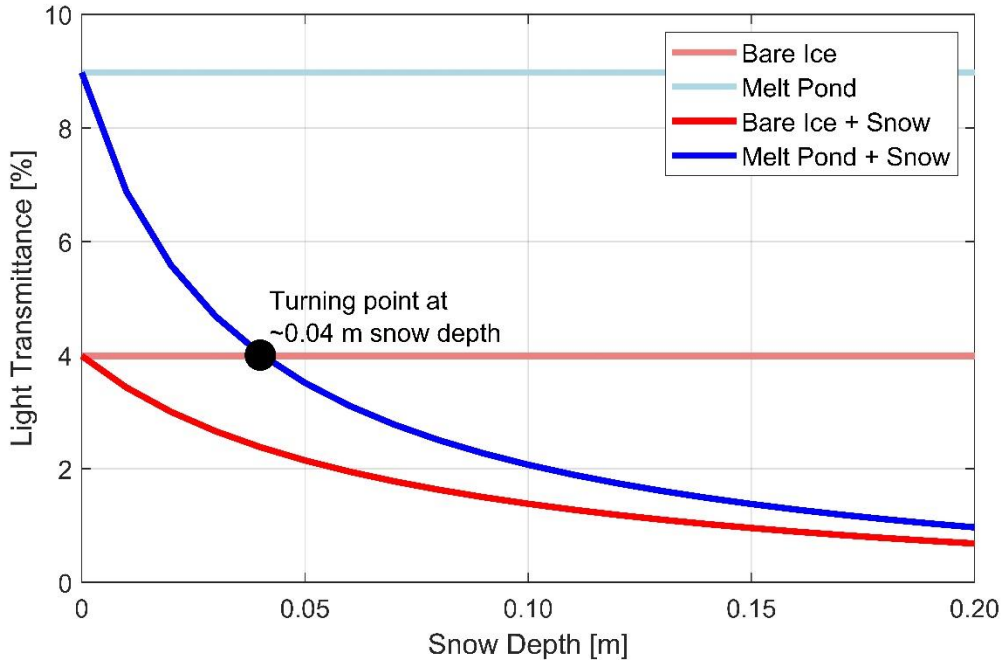

Figure S4: Simulated light transmittance depending on the snow depth as modelled by DORT2002 for four cases: bare ice (light red), melt ponds (light blue), snow-covered bare ice (red), and snow-covered melt ponds (blue).

Table S1: Parameters used in the radiative transfer model. SSL is the surface scattering layer. The melt pond depth is based on the in-situ average melt pond depth measured at six marker locations. The scattering coefficient for cold dry snow was provided by Perovich (1990). The other parameters were chosen with respect to Ehn et al. (2008), Light et al. (2008), Petrich et al. (2012b), and Katlein et al. (2021) and adjusted so that they resulted in transmittance values similar to our observations. A Henyey–Greenstein phase function with an asymmetry parameter g = 0.9 was used for all layers.

Type	Layer Thickness [m]		Scattering Coefficient [m^{-1}]	Absorption Coefficient [m^{-1}]	Refractive Index
	Bare	Pond			

Snow	0 - 0.2	0 - 0.2	800	0.15	1.33
SSL	0.1	-	250	0.15	1.33
Interior ice	2.0	1.8	25	0.15	1.33
Pond	-	0.3	0	0.10	1.30

Table S2: Statistics of measured snow depth (m), ice thickness (m), and light transmittance (%), of melt ponds and bare ice. N is the number of measurements. The modes were read from histograms (Figure 2) with bin widths of 0.01 m, 0.10 m, and 0.5 %, respectively.

Variable	Date	Type	N	Min	Max	Mean	Std	Median	Mode
Snow Depth [m]	Autumn 14.09.	Bare	1 308	0.04	0.25	0.11	0.03	0.10	0.09
		Pond	887	0.05	0.32	0.14	0.05	0.13	0.10
Ice Thickness [m]	Autumn 14.09.	Bare	26 831	1.25	2.83	1.90	0.21	1.92	2.00
		Pond	18 794	1.14	2.32	1.73	0.19	1.75	1.80
Transmittance [%]	Summer 24.08.	Bare	830	0.7	15.5	4.1	1.9	3.9	4.5
		Pond	859	1.6	23.2	8.9	5.5	7.1	5.5
	Autumn 13.09.	Bare	466	0.2	3.4	1.8	0.7	1.9	2.0
		Pond	328	0.4	3.1	1.3	0.6	1.2	1.0

References

Ehn, J. K., Papakyriakou, T. N., & Barber, D. G. (2008). Inference of optical properties from radiation profiles within melting landfast sea ice. *Journal of Geophysical Research, 113*(C09024). doi:10.1029/2007jc004656

Katlein, C., Valcic, L., Lambert-Girard, S., & Hoppmann, M. (2021). New insights into radiative transfer within sea ice derived from autonomous optical propagation measurements. *The Cryosphere*, *15*(1). doi:10.5194/tc-15-183-2021

Light, B., Grenfell, T. C., & Perovich, D. K. (2008). Transmission and absorption of solar radiation by Arctic sea ice during the melt season. *Journal of Geophysical Research, 113*(C03023). doi:10.1029/2006jc003977

Perovich, D. K. (1990). Theoretical estimates of light reflection and transmission by spatially complex and temporally varying sea ice covers. *Journal of Geophysical Research, 95*(C6). doi:10.1029/JC095iC06p09557

Petrich, C., Nicolaus, M., & Gradinger, R. (2012b). Sensitivity of the light field under sea ice to spatially inhomogeneous optical properties and incident light assessed with three-dimensional Monte Carlo radiative transfer simulations. *Cold Regions Science and Technology, 73*. doi:10.1016/j.coldregions.2011.12.004